

EBIC studies of heterojunction bipolar transistors

F Amin, D B Holt⁺, G A Hungerford*, E Napchan⁺ and A Rezazadeh

Department of Electronic Engineering, King's College London, Strand, London WC2R 2LS

⁺ Department of Materials, Imperial College of Science, Technology and Medicine, London SW7 2BP

* Present address: 6235 West Canyon Avenue, Littleton, Colorado 80123, USA

ABSTRACT: Measurements on GaAs homo- and heterojunction bipolar transistors followed the approach of Gonzales (1974) who considered the interaction of the two junctions in analysing such devices. The electron beam induced voltage produced across a charge collecting barrier without an electrical contact could be detected by a neighbouring junction. This can be useful for examining regions of integrated circuits to which no direct contact is made. Observations on the two forms of GaAs transistors are presented and discussed.

1. INTRODUCTION

Almost all published work on electron beam induced current (EBIC) deals with only one charge collection (CC) barrier i.e. with diodes. However, even the most basic of microelectronic devices, transistors, contain more than one, so the final EBIC in devices is generally the result of two or more CC processes. The results of the interactions of these barriers in planar bipolar transistors were considered by Gonzales (1974). However, no measurements related to this analysis have been published to our knowledge. This paper reports such effects in experimental GaAs homo- and hetero-junction (or heterostructure) bipolar transistors (HBTs). EBIC studies, with no reference to the work of Gonzales, were reported on GaAs HBTs (e.g. Fitzgerald et al 1988) and MESFETs (metal Schottky field effect transistors) (Kaufmann and Balk 1993). The latter measured the gate EBIC current and used simulations to achieve quantitative interpretability.

Kroemer (1957) proposed the use of a second material with a wider energy band gap for the emitter to form heterostructure bipolar transistors. Steps in the band edges limit the undesirable base-to-emitter current and make large increases in the current gain possible. HBTs are of interest for use in monolithic microwave integrated circuits (MMICs) where they compete with MESFETs and HEMTs (high electron mobility transistors) (Hughes et al 1988 pp. 403 - 418).

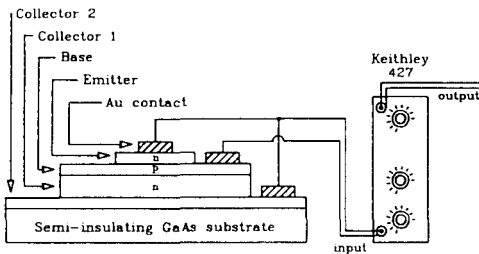
Following Gonzales' approach, Hungerford (1988) studied GaAs bipolar homojunction transistors and some of those hitherto unpublished results are reported here together with the results of recent studies of GaAs-based HBTs.

2. EXPERIMENTAL METHODS

The initial observations were on an ion-implanted, large-area (100 μm diameter) circular geometry device kindly supplied by the GEC Hirst Research Centre. The (100) GaAs for the device was grown on semi-insulating Czochralski GaAs by molecular beam epitaxy (MBE). The device was produced by photo-masking and etching as shown in the schematic cross-section diagrams of Figures 1a and 1b. It was examined in a JEOL JSM-35 SEM with a Keithley 427 amplifier to detect the EBIC signals.

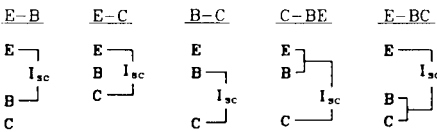
Emitter Cap	n+ GaAs 2E18 Si, 0.19 μm	
Emitter	n GaAs 2E17 Si, 0.30 μm	
Base	p+ GaAs 1E18 Be, 0.30 μm	intrinsic GaAs, 0.01 μm
Collector 1	n- GaAs 1E16 Si, 1.0 μm	
Collector 2	n+ GaAs 1E18 Si, 0.50 μm	
Super Lattice Buffer	0.195 μm intrinsic	intrinsic GaAs, 0.05 μm
		intrinsic GaAs, 0.055 μm
Semi-Insulating Cz (100) GaAs substrate		

(a)



Wiring abbreviation for configuration above E
 Mnemonic: B-EC B - I_{sc}
 C

Other wiring configurations used



(b)

Figure 1. (a) The cross-sectional structure of the homojunction transistors. (b) The six possible ways of connecting the detecting amplifier (a Keithley 427) to a bipolar transistor: configuration B-EC is shown in the main Figure. The other connection configurations are only schematically represented (Hungerford 1988).

The later devices were produced on a single chip (Figure 2) at King's College London, with the layout and structure shown in Figure 3 and Table 1. Four devices were contacted. Of these, HBTS 1 and 3 were good and HBTS 2 and 4 failed. They were examined in a JEOL JSM 840A with either a Stanford Research Systems SR570 or a Matelect ISM-5 EBIC system, operated via TestPoint software, and images were processed by a Kontron processor.

Table 1. The layer structure of the KCL HBTs.

Layer No.	Description	Material and Grading	Doping (cm^{-3})	Thickness (nm)
9	Cap layer -2	$n^+ \text{In}_{0.5}\text{Ga}_{0.5}\text{As}$	1×10^{18}	30
8	“ “ -1	$n^+ \text{In}_x\text{Ga}_{1-x}\text{As}$ ($x = 0 \Rightarrow 0.5$)	1×10^{18}	30
7	“ “	$n^+ \text{GaAs}$	8×10^{18}	100
6	“ “	$n^+ \text{In}_{0.49}\text{Ga}_{0.51}\text{P}$	8×10^{18}	30
5	Emitter	$n \text{In}_{0.49}\text{Ga}_{0.51}\text{P}$	5×10^{17}	100
4	Base	$p \text{GaAs}$	2×10^{19}	80
3	Collector	$n \text{GaAs}$	3×10^{16}	500
1	Sub-collector	$n^+ \text{GaAs}$	8×10^{18}	700
0	Substrate	Semi-insulating GaAs	Undoped	$400 \mu\text{m}$

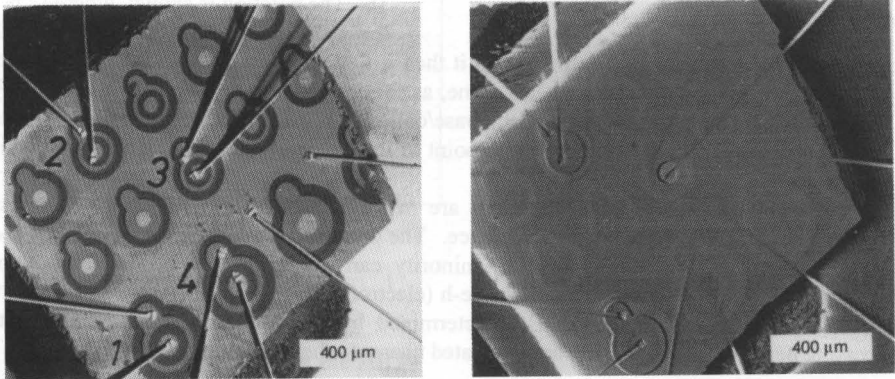


Figure 2. (a) Secondary electron and (b) EBIC images of the KCL (King's College, London) GaAs chip on a TO-18 header. HBTs 1 to 4 were connected to header pins. For (b) the EBIC system was connected to the HBT 4 emitter and a common collector contact. The other three transistors gave EBIC contrast but HBT 4, the failed device did not.

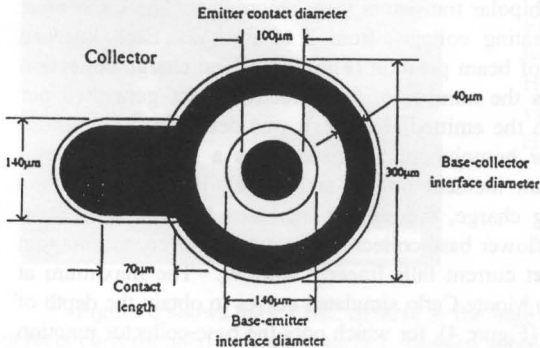


Figure 3. The layout of the KCL HBTs. The black areas are the metallization. There are two sizes of HBTs on the chip of Figure 3: the larger have $100 \mu\text{m}$ emitter contacts as indicated; the smaller have $70 \mu\text{m}$ e-contacts. The base-emitter and base-collector "interface diameters" are mesa edge positions.

2.1 EBIC ANALYSIS OF BIPOLAR TRANSISTORS

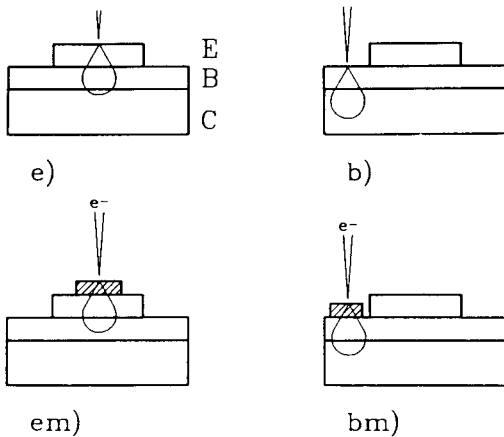


Figure 4. The four types of electron beam excitation that are possible on an unpassivated transistor: (e) electron beam on the exposed emitter layer, (b) beam on the exposed base layer, (em) on the emitter metallization and (bm) on the base metallization. (Hungerford 1988).

Different EBIC results will be expected from the contact configurations for collecting the EBIC signal in Figure 1b. The notation is shown, where I_{sc} is the short circuit (EBIC) current. If the

letter E, B or C has no wire (line) going to it then it floated electrically and the EBIC signal was taken across the other two contacts alone, as for configurations E-B, E-C and B-C. For C-BE and E-BC, the base/emitter and the base/collector respectively, were shorted together. The results also depend on the energy and point of incidence of the beam. That is, on which of the layers of the device are excited.

For E-C (Figure 1b) two junctions are in series and charge collecting in opposite directions so the EBIC signal is the difference. The dominant junction is determined by their diffusion potentials and the volume of minority carriers reaching the depletion regions (Hungerford 1988). At low beam voltages e-h (electron-hole) pairs are created in the emitter only and the direction of the EBIC is determined by the emitter-base junction. For the increasing beam voltage, e-h pairs are generated nearer to the base-collector junction.

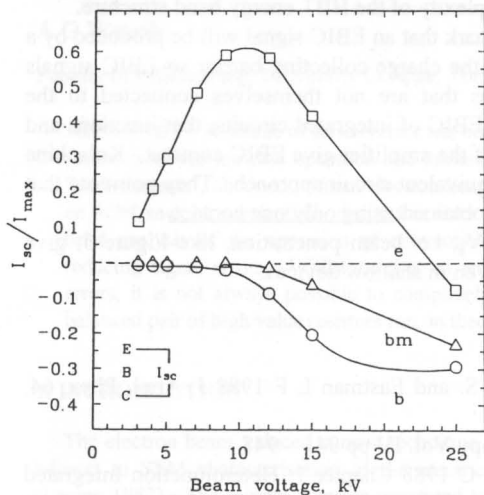
3. RESULTS

3.1 Quantitative EBIC Analysis of the Transistors

EBIC linescans across the GaAs bipolar transistors were recorded for the six contact configurations of Figure 1b, for accelerating voltages from 2 to 25 kV. Each linescan contained a signal for each of the types of beam position (Figure 4). The charge collection efficiency, i.e. the I_{sc}/I_{max} , where I_{max} is the number of hole-electron pairs generated per second (after allowing for energy lost to the emitted electrons), was determined. Figure 5 reports for contacts E-C, the results for homojunction transistors as a function of beam accelerating voltage, V_b . With the beam incident on the emitter (e), initially, when the emitter-base junction alone is collecting charge, the current increases linearly with beam energy. From about 10 kV onwards, the lower base-collector junction begins contributing an opposing current which grows so the net current falls linearly with V_b . The maximum at $V_b = 12$ kV could be fitted to (Napchan's) Monte Carlo simulated curves to obtain the depth of the lower junction. The bm and b curves (Figure 4), for which only the base-collector junction lies below the beam impact point, show that the charge collection current did indeed begin to

rise from zero, and in the opposite direction to that from the upper junction, at about 10 – 12 kV. At $V_b = 23-24$ kV, the e curve shows that the two currents are equal giving zero net EBIC signal, I_{sc} . The results for HBT1 were broadly similar.

Figure 2b is the EBIC image for connection E4-C, i.e. connection between the emitter of HBT4 and the n-type collector layer covering the whole area of the chip. All the HBTs connected to pins except the one connected to the detecting amplifier gave rise to EBIC signals. Clearly charge collection at HBTs 1 and 3 (good devices) and HBT 2 (failed - but not so completely as HBT4) was detected via the common collector. The same effect occurs



when a good device (1 or 3) is contacted but the images are dominated by the very strong signal from the good, contacted device. In Figure 2b, the absence of signal from the contacted HBT4 meant that a high amplifier gain could be used.

Figure 5. The variation of EBIC gain versus beam voltage for connection configuration E-C with the beam (e) on the emitter, (b) on the base and (bm) on the base contact metallization in the homojunction transistor (Hungerford 1988).

3.2 EBIC Defect Observations in the HBTs

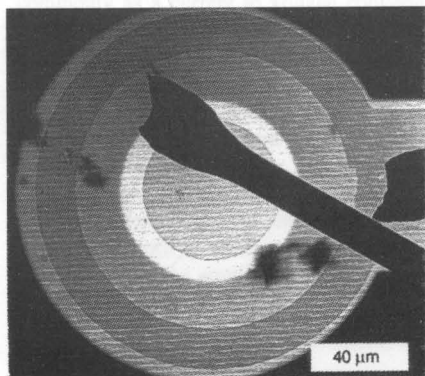


Figure 6. EBIC image of defects in the base material of one of the failed KCL HBTs (no. 2) with the signal extracted via the pins to the emitter and base of HBT 4, the other failed device.

Figure 6 shows dark EBIC defects in the base material of an HBT from KCL. These defects corresponded to visible surface damage apparently produced by the indenter used to bond the gold wire leads to the contact pads.

4. DISCUSSION

The importance of the different connection configurations (Figure 1b) and beam incidence positions (Figure 4) is clear. However, measurements showed many of the connection configurations produce similar results (Hungerford 1988). For connections E-C the two junctions work in opposition to produce the forms of beam accelerating voltage dependence shown in Figures 5. The form of Figure 5 could be simply understood as discussed above. However, the interpretation of the form of the similar curve for the heterojunction devices involves the greater complexity of the HBT energy band structure.

Figure 2b supports Gonzales' (1974) remark that an EBIC signal will be produced by a neighbouring junction that injects carriers into the charge collecting barrier so EBIC signals can be picked up from junctions and devices that are not themselves connected to the detecting amplifier. It has often been found in EBIC of integrated circuits, that junctions and devices, remote from the points of connection of the amplifier give EBIC contrast. Kolachina et al (1998) have treated such a case using an equivalent circuit approach. They point out that EBIC images of integrated circuits can even be obtained using only one contact.

Maxima in plots of EBIC gain versus V_b , i.e. beam penetration, like Figure 5, give information about the depths of the junctions, even in shallow devices.

REFERENCES

- Fitzgerald E A, Ast D G, Ashizawa Y, Akbar S. and Eastman L F 1988 J. Appl. Phys. **64**, 2473
- Gonzales A J 1974 Scanning Electron Microscopy Vol. IV pp 941 – 948
- Hughes W A, Rezazadeh A A and Wood C E C 1988 Chapter 7: Heterojunction Integrated Circuits; in GaAs Integrated Circuits (J. Mun, Editor) (BSP Professional Books: Oxford) pp 376 - 429
- Hungerford G A 1988 Ph.D. Thesis, University of London
- Kaufmann K and Balk L J 1993 in Microscopy of Semiconducting Materials. Inst. Phys. Conf. Ser. **134** (Inst. Phys.: Bristol) pp 725 – 730
- Kolachina S, Phang J C H and Chan D S H 1998 Sol.-State Electron. **42**, 957
- Kroemer H 1957 Proc. IRE **45**, 1535